



MSC: 76N15, 35L45

Approximate solution to the Riemann problem in non-classical gas dynamics

M. R. Koroleva

Udmurt Federal Research Center

of the Ural Branch of the Russian Academy of Sciences,

34, T. Baramzina str., Izhevsk, 426067, Russian Federation.

Abstract

This study considers an approach to construct an approximate solver for the non-classical Riemann problem. In this regime, the solution of the discontinuity decay problem may contain composite waves, including both classical and non-classical compression and rarefaction waves. The algorithm for finding the exact solution is based on a geometric representation of shock and rarefaction waves on isentropic curves and involves the repeated use of iterative methods to solve local tasks, such as identifying inflection points on isentropes, points of tangency between a straight line and a curve, intersection points, and others. A significant challenge when using iterative methods is the need to specify initial guesses that ensure method convergence. The approach proposed in this work is based on tabulating exact solutions for Riemann problems over a wide range of initial state parameters. These tabulated data are then used to find an approximate solution without requiring iterative methods. The approximate solver was successfully applied to solve two one-dimensional discontinuity decay problems in the non-classical domain.

Keywords: Riemann problem, non-classical gas dynamics, exact solution, approximate solution, solution geometric interpretation, tabulated data.




Received: 26th February, 2025 / Revised: 5th April, 2025 /

Accepted: 28th April, 2025 / First online: 2nd September, 2025

Mathematical Modeling, Numerical Methods and Software Complexes Research Article

© The Author(s), 2025

© Samara State Technical University, 2025 (Compilation, Design, and Layout)

   The content is published under the terms of the [Creative Commons Attribution 4.0 International License](http://creativecommons.org/licenses/by/4.0/) (<http://creativecommons.org/licenses/by/4.0/>)

Please cite this article in press as:

Koroleva M. R. Approximate solution to the Riemann problem in non-classical gas dynamics, *Vestn. Samar. Gos. Tekhn. Univ., Ser. Fiz.-Mat. Nauki* [J. Samara State Tech. Univ., Ser. Phys. Math. Sci.], 2025, vol. 29, no. 3, pp. 503–515. EDN: [ASUEIW](https://orcid.org/0000-0001-5697-9199). DOI: [10.14498/vsgtu2166](https://doi.org/10.14498/vsgtu2166).

Author's Details:

Mariya R. Koroleva   <https://orcid.org/0000-0001-5697-9199>

Cand. Phys. & Math. Sci.; Senior Researcher; Institute of Mechanics; e-mail: koroleva@udman.ru

1. Introduction. Exact solutions to the fluid dynamics equations are important for several reasons. First, they provide a convenient tool for the theoretical study of liquid and gas flow characteristics [1–3]. Furthermore, exact solutions are widely used for verifying new numerical models developed to approximate solutions to fluid dynamics problems [4, 5]. They are particularly relevant for complex and generally underexplored physical regimes, such as those in non-classical gas dynamics.

Non-classical gas dynamics is a field of fluid mechanics that studies the dynamic behavior of substances not obeying the ideal gas law. Such substances include, for example, dense gases, supercritical compressible fluids, and certain two-phase media. These gases, referred to as real gases, are described by special equations of state and are characterized by thermodynamic conditions near the saturation curve in the region where the fundamental derivative G is negative [6–8]:

$$G(p, v) = \frac{v^3}{2c^2} \left(\frac{\partial^2 p}{\partial v^2} \right)_s,$$

where p is pressure, v is specific volume, and $c = \sqrt{-v^2(\partial p/\partial v)_s}$ is the speed of sound evaluated along an isentrope $s = \text{const}$.

The region with $G < 0$ is termed the inversion zone. In Fig. 1, the inversion zone is highlighted in gray on the $(p-v)$ diagram. In this region, the wave structure of the Riemann problem solution is non-trivial, involving unusual phenomena such as rarefaction shocks and smooth compression fans [9, 10]. These can also combine to form complex composite waves known as non-classical waves. The emergence of non-classical waves is related to the convexity of the isentropes on the $(p-v)$ diagram and the relative position of the contact discontinuity with respect to the initial states in the Riemann problem.

To find the exact solution to the Riemann problem in the inversion zone, a complex geometric algorithm proposed in [7] can be applied. This algorithm requires solving a series of local problems: (a) finding the inflection points of the isentropes, (b) constructing the tangent lines at the curve points, (c) determining the intersection points of a curve with a secant line, and (d) solving a nonlinear system of equations. This approach is justified for a simple test problem. However,

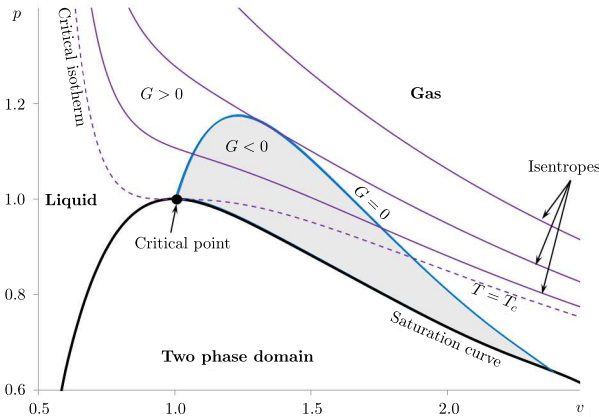


Figure 1. $(p-v)$ diagram close to the critical point; the inversion zone ($G < 0$) is shaded in gray

it becomes impractical for larger-scale applications, even in one dimension. The local problems listed above are typically solved iteratively using Newton's method, which is highly sensitive to the initial approximation, particularly in the inversion region [11].

In this study, a method for constructing an approximate Riemann solver for non-classical gas dynamics in the inversion region is proposed. It is based on the exact solution of the Riemann problem but is less computationally intensive while still capturing the essential features of the non-classical solution.

2. Geometric Interpretation of the Riemann Problem Solution. Let us consider the Riemann problem for the Euler equations governing the motion of a compressible inviscid non-heat-conducting gas. To construct the solution, the specific volume v , the velocity u , and the specific entropy s are used as the unknown variables. By introducing the definitions

$$W = \begin{pmatrix} v \\ u \\ s \end{pmatrix}, \quad A(W) = \begin{pmatrix} u & -v & 0 \\ v \left(\frac{\partial p}{\partial v} \right)_s & u & v \left(\frac{\partial p}{\partial s} \right)_v \\ 0 & 0 & u \end{pmatrix},$$

the governing gasdynamic equations can be written as follows:

$$\frac{\partial W}{\partial t} + A(W) \frac{\partial W}{\partial x} = 0. \quad (1)$$

The system of equations (1) is closed by an equation of state in the general form $e = e(s, v)$, from which the gas pressure $p(s, v)$ can be determined.

The initial data contain a discontinuity separating two states with uniform distributions on the left and right sides:

$$W(x, 0) = \begin{cases} W_{\text{Left}}, & \text{for } x < 0, \\ W_{\text{Right}}, & \text{for } x > 0, \end{cases}$$

where $W_{\text{Left}} = (p_L, v_L, u_L)$ and $W_{\text{Right}} = (p_R, v_R, u_R)$. To find the solution, the intermediate state $W_{\text{indt}} = (p^*, v_L^*, v_R^*, u^*)$ that connects W_{Left} and W_{Right} must be determined.

In classical gas dynamics, the Riemann problem has a self-similar solution comprising a system of simple waves—shock waves (s) or rarefaction waves (f)—connected by a contact discontinuity (cd). In general, a set of possible solutions, or *solution patterns*, can be denoted as follows: s – s , s – f , f – s , f – f . The wave structure of the solution depends on the intermediate state (p^*, v_L^*, v_R^*, u^*) , obtained by determining the intersection between the one-parameter family of states connected to the left state (p_L, v_L) and the one-parameter family associated with the right state (p_R, v_R) .

One of the solutions is shown in Fig. 2. It includes, from left to right, a rarefaction wave, a contact discontinuity, and a shock wave. The solution is characterized by an f – s pattern, sketched in Fig. 2, *b*. This corresponds to Sod's shock tube problem with the initial data:

$$\text{Sod: } \begin{cases} v_L = 1, & p_L = 1, & u_L = 0, \\ v_R = 8, & p_R = 0.1, & u_R = 0. \end{cases}$$

In Fig. 2, a, two isentropes are shown on the $(p-v)$ diagram: the lower one corresponds to the gas parameters on the left of the discontinuity, and the upper one to the gas parameters on the right. The line denoted as s_{RH} is the Hugoniot adiabat. The red composite line connecting these two states represents the solution to the Riemann problem. Since $p_L > p^*$, the solution on the left side contains a rarefaction wave. On the right side, $p_R < p^*$; therefore, a shock wave forms there. These waves are connected by a contact discontinuity. The pressure, specific volume, and velocity distributions are shown in Fig. 2, c, d, and e, respectively.

The pressure value in the intermediate state p^* is defined by the equation $F(p) = 0$ [11]. This equation arises from a combination of the Rankine–Hugoniot relations and the condition of constant entropy. For an ideal gas, $F(p)$ can be expressed in terms of pressure and velocity variables, without the specific volume variable, as follows:

$$F(p) = f(p, p_L, v_L) + f(p, p_R, v_R) - (u_L - u_R) = 0. \quad (2)$$

The functions $f(p, p_L, v_L)$ and $f(p, p_R, v_R)$ in (2) are defined as:

$$f(p, p_H, v_H) = \begin{cases} \frac{(p - p_H)v_H}{c_H \sqrt{\frac{\gamma+1}{2\gamma} \frac{p}{p_H} + \frac{\gamma-1}{2\gamma}}}, & \text{for } p \geq p_H, \\ \frac{2}{\gamma-1} c_H \left[\left(\frac{p}{p_H} \right)^{\frac{\gamma-1}{2\gamma}} - 1 \right], & \text{for } p < p_H, \end{cases}$$

where the subscript “H” denotes “L” for the left wave and “R” for the right wave,

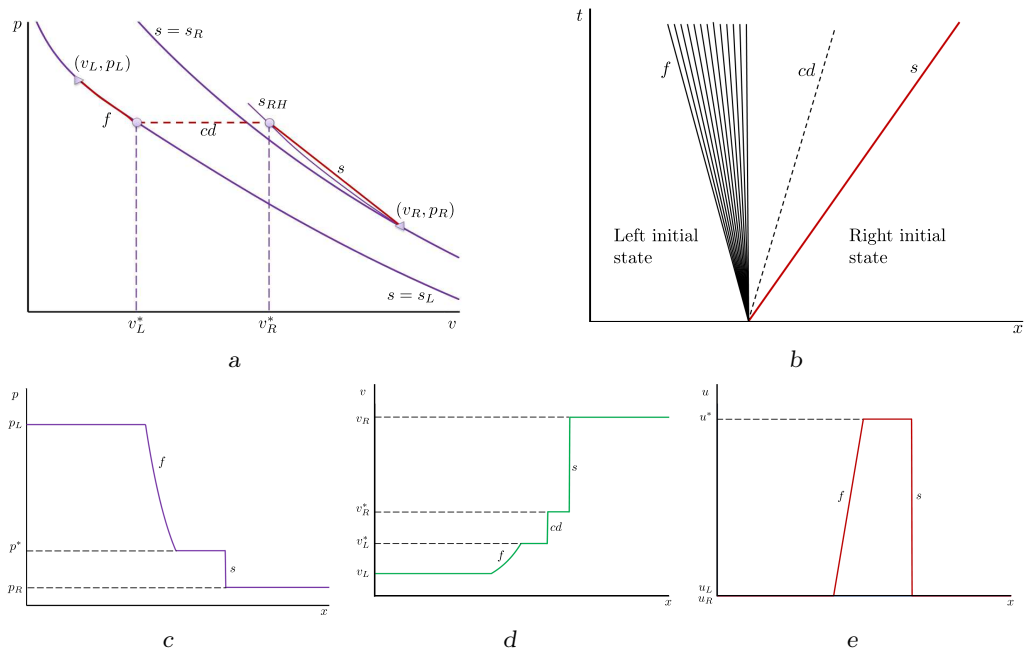


Figure 2. Schematic of the Riemann problem solution for the fan–shock case in classical gas dynamics: a) $(p-v)$ plane; b) characteristic field; c) pressure distribution; d) specific volume distribution; e) velocity distribution

γ is the specific heat ratio, and c_H is the speed of sound, calculated from the equation of state.

In non-classical gas dynamics, the isentropes corresponding to the left and right initial states can exhibit concave portions. The algorithm proposed in [7] is based on a geometric procedure that requires constructing the convex envelope for a set of points in the $(p-v)$ plane. This construction can be viewed as a method to connect two states in the $(p-v)$ plane by combining different paths—portions of the flux curve and straight-line segments. The result is a composite curve with no convexity changes. The shape of this composite curve between the two states determines the resulting wave type. This algorithm is physically justified by the Oleinik entropy condition [12]. Constructing the solution requires determining the following elements for each isentrope:

- 1) Two inflection points: $(p_L^i, v_L^i)_{1,2}$ and $(p_R^i, v_R^i)_{1,2}$;
- 2) Two absolute envelope points: $(p_L^e, v_L^e)_{1,2}$ and $(p_R^e, v_R^e)_{1,2}$;
- 3) Points where a straight line is tangent to the isentrope: (p_L^t, v_L^t) , (p_R^t, v_R^t) , and (p_v^t, v_v^t) ;
- 4) Points where a straight line intersects the isentrope: $(p^{\text{inter}}, v^{\text{inter}})$.

In this case, the solution can include both classical waves (rarefaction fans and shock waves) and non-classical waves (compression fans (F) and rarefaction shocks (S)). Moreover, the solution may involve composite waves, such as a non-classical rarefaction shock combined with a classical rarefaction fan from the left state, and a classical shock combined with a non-classical compression fan and a classical shock from the right state (e.g., an $Sf-sFs$ pattern).

Let us consider two test examples with non-classical wave solutions for the Riemann problem, with the following initial conditions:

$$f-F \text{ case: } \begin{cases} v_L = 0.677, & p_L = 1.405, & u_L = -0.1365, \\ v_R = 1.451, & p_R = 1.03, & u_R = -0.1. \end{cases} \quad (3)$$

$$Fs-f \text{ case: } \begin{cases} v_L = 1.294, & p_L = 0.959, & u_L = 0, \\ v_R = 1.423, & p_R = 1.055, & u_R = 0. \end{cases} \quad (4)$$

The general solution for the initial state (3) has an $f-F$ pattern. Its left part is a classical rarefaction fan. Since the right state lies within the inversion zone on the $(p-v)$ diagram, the solution includes a non-classical wave—a compression fan. A schematic of the solution for the initial conditions (3) from the right state is shown in Fig. 3, a. The coordinate v_R^* of the intermediate state point is located between the inflection points v_R^{i1} and v_R^{i2} of the right isentrope. Thus, a non-classical compression fan wave forms, highlighted in red in Fig. 3.

The general solution for the initial state (4) has an $Fs-f$ pattern. The left initial state also lies within the inversion zone. A schematic of the solution for the initial conditions (4) from the left state is shown in Fig. 3, b. The coordinate v_L^* of the intermediate state point is located ahead of the inflection points v_L^{i1} and v_L^{i2} of the left isentrope. However, a straight line is required to connect v_L^* with the non-classical rarefaction shock originating from the left state.

The pressure and gas velocity for intermediate state of the solution are determined from the nonlinear system of two equations imposing that both pressure and velocity assume the same values across the contact discontinuity.

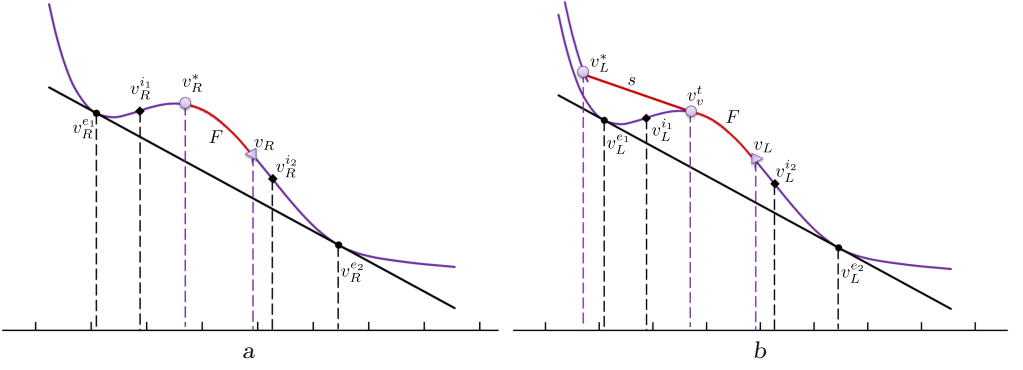


Figure 3. Schematic of the Riemann problem solution for non-classical gas dynamics: a) F -wave pattern from the right initial state for the f - F case; b) Fs -wave pattern from the left initial state for the Fs - f case

$$\begin{cases} p(v_L^*, p_L, v_L) = p(v_R^*, p_R, v_R), \\ u(v_L^*, p_L, v_L, u_L) = p(v_R^*, p_R, v_R, u_R). \end{cases} \quad (5)$$

The solution of the equation system (5) is determined by the relations for pressure and velocity as functions of v for different wave structures. It is necessary to use expressions for the sound speed, gas velocity, and pressure for the rarefaction wave, along with the Hugoniot relations for shock waves [8]. These equations depend on the equation of state. For a van der Waals gas [13], the general expressions can be written as follows:

– Pressure for the rarefaction wave:

$$Q(v, p_H, v_H) = \left(p_H + \frac{1}{v_H^2} \right) \left(\frac{v_H - 1}{v - 1} \right)^{1+\delta} - \frac{1}{v^2}; \quad (6)$$

– Pressure for the shock wave:

$$p^{RH}(v, p_H, v_H) = \frac{e_H - p_H \frac{v - v_H}{2} + \left(1 - \frac{1}{\delta} \right) \frac{1}{v} + \frac{1}{\delta v^2}}{\left(\frac{1}{2} + \frac{1}{\delta} \right) v - \left(\frac{1}{2} v_H + \frac{1}{\delta} \right)}. \quad (7)$$

In (6) and (7), $\delta = R/c_v$ is a dimensionless parameter, where c_v is the specific heat at constant volume and R is the gas constant of the substance. There exists a boundary value $\delta_{\text{nonclas}} = 0.06$; substances with δ below this value exhibit behavior within the inversion zone. The problems (3) and (4) have been formulated for $\delta = 0.008$, and the relations (6) and (7) have been used to define the functions in (5):

– For shock waves:

$$\begin{cases} p(v, p_H, v_H) = p^{RH}(v, p_H, v_H) = p^{RH}, \\ u(v, p_H, v_H, u_H) = u_H \mp z \cdot \sqrt{(v_H - v)(p^{RH} - p_H)}, \\ z = \text{sign}(v_H - v); \end{cases} \quad (8)$$

– For rarefaction fans:

$$\begin{cases} p(v, p_H, v_H) = Q(v, p_H, v_H), \\ u(v, p_H, v_H, u_H) = u_H \pm \int_{v_H}^v \sqrt{-Q'(v, p_H, v_H)} dv, \\ Q'(v, p_H, v_H) = \frac{\partial Q(v, p_H, v_H)}{\partial v}; \end{cases} \quad (9)$$

– For non-classical double composite waves (*fs* construction):

$$\begin{cases} p(v, p_H, v_H) = p^{RH}(v, p_v^t, v_v^t) = p_v^{RH}, \\ p_v^t = Q(v_v^t, p_H, v_H), \\ u(v, p_H, v_H, u_H) = u_H \pm \int_{v_H}^{v_v^t} \sqrt{-Q'(v, p_H, v_H)} dv - \\ \quad - z \cdot \sqrt{(v_v^t - v)(p_t^{RH} - p_v^t)}, \\ z = \text{sign}(v_v^t - v). \end{cases} \quad (10)$$

Similar expressions can be derived for all possible wave patterns in accordance with the wave solution identification algorithm.

3. Constructing the Solution for Composite Waves. Constructing the solution for composite waves requires considering all possible wave patterns over a wide range of the variable v in the system (5). To build the solution, specific volume-dependent Boolean variables must be defined:

- 1) A procedure for selecting the correct wave associated with the left initial state begins by determining the location of the left point on the isentrope. If the wave starts with a segment along the isentrope, the first logical variable is true (**PrL = true**). Otherwise, **PrL = false**.
- 2) To identify a classical rarefaction fan or a non-classical compression fan, the local coordinate v must be positioned relative to the inflection points. If the segment (v_L, v) does not contain any inflection point, the second logical variable is true (**PrInf = true**).
- 3) To define the non-classical *fS* and *fSf* patterns, the location of v relative to the absolute envelope points must be identified. If the segment (v_L, v) contains both absolute envelope points, the third logical variable is false (**PrAbs = false**).
- 4) To identify the non-classical *S* and *Sf* patterns, the position of the isentrope curve relative to the secant line through (v_L, p_L) and $(v, p(s_L, v))$ must be determined. If the segment lies above the curve, the fourth logical variable is true (**PrSecUp = true**).
- 5) To define a shock wave (*s*) or double non-classical *SF* and *sFs* patterns, the position of the isentrope curve relative to the secant line through (v_L, p_L) and $(v, p(s_L, v))$ must be determined. If the segment lies below the curve, the fifth logical variable is true (**PrSecDn = true**).
- 6) To identify the non-classical *SF* and *sFs* patterns, the local coordinate v must be positioned relative to the inflection points. If the segment (v, v_L^t) does not contain any inflection point, the sixth logical variable is true (**PrInfT = true**).

These Boolean variables are not used simultaneously, but the logical structure of the algorithm cannot be constructed without all of them. The DRAKON flowchart [14] of the algorithm for wave solution identification is presented in Fig. 4. It is designed for the left initial state when $v_L < v$. The DRAKON flowchart for the left initial state when $v_L > v$ is presented in Fig. 5.

The input data for this algorithm are the initial state parameters (p_L, v_L) and the variable v . Depending on the current value of v , one of five different wave patterns from the left side must be selected. A similar procedure applies to the right wave solution. The presented algorithm is used to define the complicated functions in the system (5).

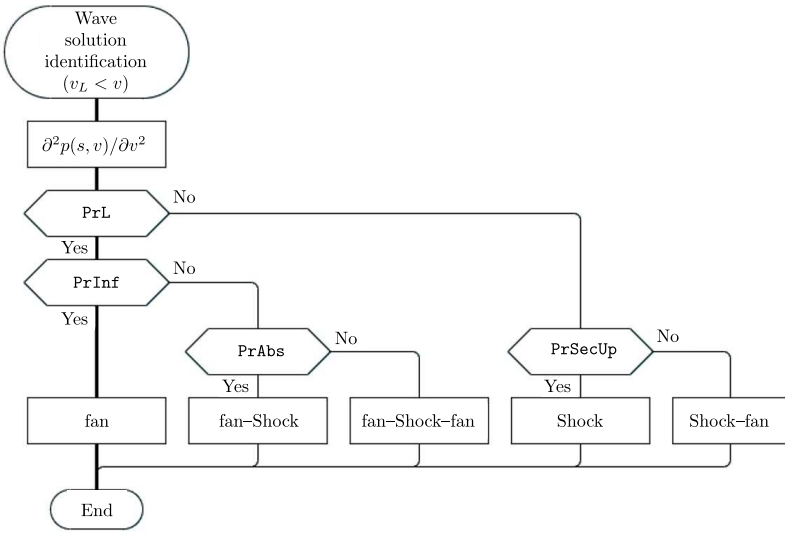


Figure 4. DRAKON flowchart of the algorithm for wave solution identification ($v_L < v$)

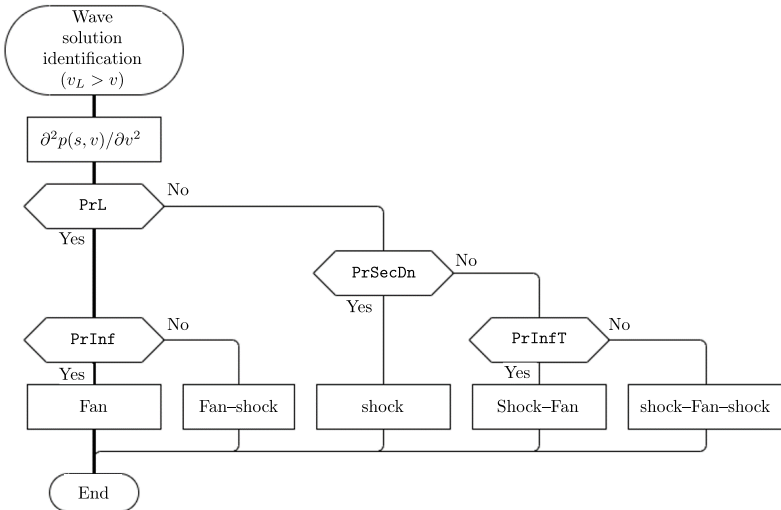


Figure 5. DRAKON flowchart of the algorithm for wave solution identification ($v_L > v$)

4. Approximate Solution. The system (5) can be solved by any iterative method; for example, Newton's method can be applied. The existence and uniqueness of the solution to the Riemann problem have been established for classical gas dynamics [15, 16], but this has not been rigorously formulated for the non-classical regime. Moreover, iterative methods are also required to solve various nonlinear equations for determining:

- inflection points;
- absolute envelope points;
- points of tangency between a straight line and an isentrope curve;
- points of intersection between a straight line and an isentrope curve.

In the field of non-classical gas dynamics, these functions, as well as those in (5), are composite, and the problem of specifying a suitable initial guess for iterative methods arises. This issue becomes particularly acute at the junctions of waves in a composite solution, where iterative methods often diverge. Numerical experiments have shown that for solving the aforementioned problems, the bisection method is more robust. However, even using the bisection method, in some cases, “manual” control of the solution search procedure is required. The application of iterative methods to the Riemann problem in non-classical gas dynamics is justified for simple test problems. However, it becomes impractical for larger-scale applications, such as when used as a building block within the Godunov method. Extending the algorithm to a three-dimensional statement on a non-orthogonal grid results in a physically justified but computationally inefficient algorithm from a practical implementation perspective.

Given the above situation, an approximate Riemann solver appears to be a viable alternative. The approach proposed in the present study to construct an approximate Riemann solver is based on approximating the complex functions in (5) without relying on specific initial states. Four different approaches have been employed to build approximate solvers within the Godunov method framework in [17]: linearization of the nonlinear equations, cubic interpolation, local approximation of the equation of state using a two-term equation of state [11, 17], and a tabulation method. Analysis of the obtained results demonstrated the effectiveness of two approaches: the local approximation method and the tabulation method. In this work, the tabulation method is applied to solve problems (3) and (4).

The key challenge with composite wave solutions is the inability to express pressure analytically as a function of gas velocity, as is achieved for the ideal gas in equation (2). The main idea of the proposed approach is to replace the governing continuous functions of the solution with their discrete representations at interpolation nodes. These discrete functions can then be used to solve the Riemann problem both in isolation, for test problems, and as part of the Godunov method for more complex problems.

For this purpose, three interpolation meshes are defined:

$$\begin{cases} p_H^i = p_H^{i-1} + \Delta p_i, & i = \overline{1, N_p}, & p_H^0 = p_H^{\min}, & p_H^{N_p} = p_H^{\max}, \\ v_H^j = v_H^{j-1} + \Delta v_j, & j = \overline{1, N_v}, & v_H^0 = v_H^{\min}, & v_H^{N_v} = v_H^{\max}, \\ v_k = v_{k-1} + \Delta v_k, & k = \overline{1, N}, & v^0 = v_{\min}, & v^N = v_{\max}. \end{cases} \quad (11)$$

Here, Δp_i , Δv_j , and Δv_k are the step sizes of the interpolation mesh for the initial pressure, initial specific volume, and specific volume variable, respectively;

N_p , N_v , and N are the numbers of nodes in the interpolation mesh.

For each point on these meshes, the discrete values $p_{i,j} = p(v, p_H^i, v_H^j)$ and $\Delta u_{i,j} = \Delta u(v, p_H^i, v_H^j)$ are computed at all points v_k using equations (8), (9), and (10). Suppose the initial state (p_L, v_L) of a given problem falls within the intervals $p_H^{i-1} < p_L < p_H^i$ and $v_H^{j-1} < v_L < v_H^j$. The values of the functions $p(v, p_L, v_L)$ and $\Delta u(v, p_L, v_L, u_L)$ at the points v_k can be obtained using bilinear interpolation. In Fig. 6, five lines in the $(p-v)$ plane are shown. The dashed lines represent the pressure functions defined on the interpolation meshes (11), and the solid line represents the pressure function obtained by bilinear interpolation for the given values (p_L, v_L) . The velocity function is determined similarly.

In general, the solution to the Riemann problem is based on the functions $p_1(v) = p(v, p_L, v_L)$, $p_2(v) = p(v, p_R, v_R)$ and $u_1(v) = u_L - \Delta u(v, p_L, v_L)$, $u_2(v) = u_R + \Delta u(v, p_R, v_R)$, defined on the set of values v_k . These functions satisfy the system (5). A graphical representation of the Riemann problem solution is shown in Fig. 7.

To find the solution, two values v_L^* and v_R^* must be determined such that the following equalities hold:

$$p_1(v_L^*) = p_2(v_R^*),$$

$$u_1(v_L^*) = u_2(v_R^*).$$

Since the functions under consideration are discrete, a non-iterative procedure can be employed to find the solution. For this purpose, it is necessary to construct the discrete function $P(u) = p_1^*(u) - p_2^*(u)$ on the common interval of the variable u , thereby eliminating the variable v from the relations. This is feasible for every pair of discrete functions:

$$p_1(v), u_1(v) \Rightarrow p_1^*(u),$$

$$p_2(v), u_2(v) \Rightarrow p_2^*(u),$$

as they are defined on the same interpolation points.

In this case, solving the system (5) becomes unnecessary. The solution can be directly determined on the interval $[u_{i-1}, u_i]$ where the function $P(u)$ changes

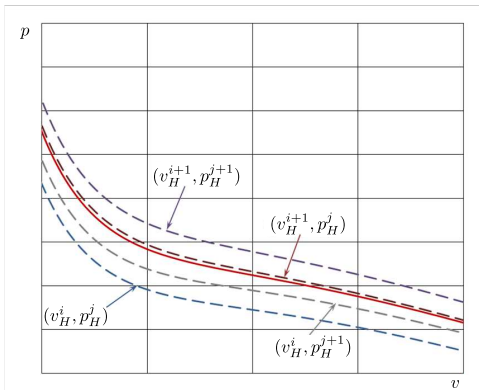


Figure 6. Bilinear interpolation for the solution function

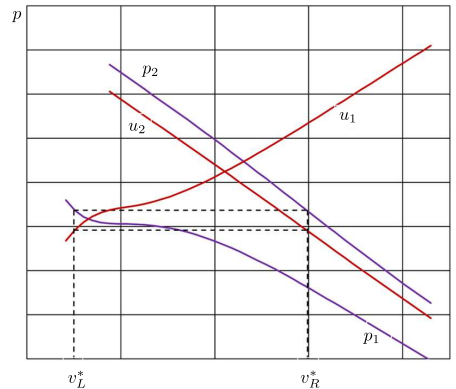


Figure 7. Solution construction

sign. Assuming a linear variation of $P(u)$ between the mesh nodes u_{i-1} and u_i , the gas velocity at the contact discontinuity is found using the formula:

$$u^* = u_i - P(u_i) \frac{u_i - u_{i-1}}{P(u_i) - P(u_{i-1})}.$$

Knowing the velocity u^* , the pressure at the contact discontinuity can be calculated from either of the two functions— $p_1^*(u)$ or $p_2^*(u)$. Then, the specific volume values v_L^* and v_R^* are uniquely determined from the corresponding tabulated functions.

The described approach has been applied to approximately solve the test problems (3) and (4). A comparison of the exact solution of these problems with the approximate one is given in Table 1. The maximum absolute deviation of the approximate solution from the exact one does not exceed 0.06.

Table 1
Comparison of exact and approximate solutions for the test problems

Parameter	Solution	
	Exact	Approximate
<i>f</i> – <i>F</i> case		
p^*	1.09759974969995	1.09763372318514
u^*	−0.159809461904289	−0.159716582534566
v_L^*	0.903652908743441	0.903792866716065
v_R^*	1.16005152731677	1.15985386107073
<i>F</i> – <i>f</i> case		
p^*	0.991790383560825	0.991866646053808
u^*	−0.122048393289314	−0.121922929652812
v_L^*	0.83579973857623	0.835319156613279
v_R^*	1.65865734349481	1.65845846192419

5. Conclusion. In the present paper, an approach to construct an approximate solver for the Riemann problem in the non-classical regime of gas dynamics is proposed. It is based on utilizing tabulated discrete data obtained from the exact solutions of the discontinuity decay problem on an interpolation mesh. This approach eliminates the need for iterative methods to find an approximate solution and allows for the correct identification of physical quantities in composite wave solutions.

Competing interests. The author declares no competing interests.

Author’s Responsibilities. The author takes full responsibility for the content of the manuscript and the decision to submit the final version for publication.

Funding. This research did not receive any specific grant from funding agencies in the public, commercial, or not-for-profit sectors.

References

1. Deville M. O. Exact solutions of the Navier–Stokes Equations, In: *An Introduction to the Mechanics of Incompressible Fluids*, vol. 22. Cham, Springer, 2022, pp. 51–89. DOI: https://doi.org/10.1007/978-3-031-04683-4_3.
2. Nikonorova R., Siraeva D., Yulmukhametova Y. New exact solutions with a linear velocity field for the gas dynamics equations for two types of state equations, *Mathematics*, 2022, vol. 10, no. 1, 123. EDN: [FSXDCX](https://doi.org/10.3390/math10010123). DOI: <https://doi.org/10.3390/math10010123>.

3. Prosviryakov E. Yu., Ledyankina O. A., Goruleva L. S. Exact solutions to the Navier–Stokes equations for describing the flow of multicomponent fluids with internal heat generation, *Russ. Aeronaut.*, 2024, vol. 67, no. 1, pp. 60–69. EDN: **CLAH0C**. DOI: <https://doi.org/10.3103/S1068799824010070>.
4. Brutyani M. A., Ibragimov U. G. Exact solution of the Navier–Stokes equations for rotational tornado-like flow of a viscous gas, *Proc. Moscow Inst. Phys. Technol.*, 2024, vol. 16, no. 3(63), pp. 92–104 (In Russian). EDN: **FPNPCE**.
5. Galkin V. A., Dubovik A. O., Morgun D. A. Visualization of flow of a viscous incompressible fluid corresponding to exact solutions of the Navier–Stokes equations, *Sci. Vis.*, 2024, vol. 16, no. 1, pp. 52–63 (In Russian). EDN: **NWGODH**. DOI: <https://doi.org/10.26583/sv.16.1.05>.
6. Guardone A., Vigeveno L., Argrow B. M. Assessment of thermodynamic models for dense gas dynamics, *Phys. Fluids*, 2004, vol. 16, no. 11, pp. 3878–3887. DOI: <https://doi.org/10.1063/1.1786791>.
7. Fossati M., Quartapelle L. *The Riemann problem for hyperbolic equations under a nonconvex flux with two inflection points*, 2014, arXiv: [1402.5906](https://arxiv.org/abs/1402.5906) [physics.flu-dyn].
8. Quartapelle L., Castelletti L., Guardone A., Quaranta G. Solution of the Riemann problem of classical gasdynamics, *J. Comput. Phys.*, 2003, vol. 190, no. 1, pp. 118–140. DOI: [https://doi.org/10.1016/S0021-9991\(03\)00267-5](https://doi.org/10.1016/S0021-9991(03)00267-5).
9. Coquelet C., Chapoy A., Richon D. Development of a new alpha function for the Peng–Robinson equation of state: Comparative study of alpha Function models for pure gases (natural gas components) and water-gas systems, *Int. J. Thermophys.*, 2004, vol. 25, no. 1, pp. 133–158. DOI: <https://doi.org/10.1023/b:ijot.0000022331.46865.2f>.
10. Qi J., Xu J., Han K., et al. Development and validation of a Riemann solver in Open-FOAM® for non-ideal compressible fluid dynamics, *Eng. Appl. Comput. Fluid Mech.*, 2022, vol. 16, no. 1, pp. 116–140. DOI: <https://doi.org/10.1080/19942060.2021.2002723>.
11. Godunov S. K., Zabrodin A. V., Ivanov M. Ya., et al. *Chislennoe reshenie mnogomernykh zadach gazovoi dinamiki* [Numerical Solution of Multidimensional Problems in Gas Dynamics]. Moscow, Nauka, 1976, 401 pp. (In Russian)
12. Glass O. An extension of Oleinik’s inequality for general 1D scalar conservation laws, *J. Hyperbolic Differ. Equ.*, 2008, vol. 5, no. 1, pp. 113–165. DOI: <https://doi.org/10.1142/S0219891608001398>.
13. Zhang L., Gao G. Equations of states and polytropic processes of van der Waals gases, *Phys. Eng.*, 2024, vol. 34, no. 3, pp. 16–21. DOI: <https://doi.org/10.26599/PHYS.2024.9320303>.
14. Parondzhanov V. D., Mitkin S. B. The DRAKON medical algorithmic language and the DRAKON-builder program for the creation and application of clinical algorithms, *Virtual Technol. Med.*, 2022, no. 1, pp. 32–44 (In Russian). EDN: **YKCSIC**. DOI: https://doi.org/10.46594/2687-0037_2022_1_1410.
15. Liu T.-P. The Riemann problem for for general systems of conservation laws, *J. Differ. Equ.*, 1975, vol. 18, no. 1, pp. 218–234. DOI: [https://doi.org/10.1016/0022-0396\(75\)90091-1](https://doi.org/10.1016/0022-0396(75)90091-1).
16. Smith R. G. The Riemann problem in gasdynamics, *Trans. Amer. Math. Soc.*, 1979, vol. 249, no. 1, pp. 1–50. DOI: <https://doi.org/10.1090/S0002-9947-1979-0526309-2>.
17. Koroleva M. R., Tenenev V. A. Approximate Riemann solvers for the Soave–Redlich–Kwong equation of state, *Russ. J. Nonlinear Dyn.*, 2024, vol. 20, no. 3, pp. 345–359. EDN: **KFCNYJ**. DOI: <https://doi.org/10.20537/nd240905>.

УДК 517.958:531.332

Приближенное решение задачи Римана для неклассической газовой динамики

М. Р. Королева

Удмуртский федеральный исследовательский центр
Уральского отделения Российской академии наук,
Россия, 426067, Ижевск, ул. Т. Барамзиной, 34.

Аннотация

Рассмотрен подход к построению приближенного решателя для неклассической задачи Римана. Решение задачи о распаде разрыва в области неклассической газовой динамики может содержать составные волны, включающие чередующиеся волны сжатия и разрежения, в том числе неклассические. Алгоритм нахождения точного решения строится на основе геометрического представления ударных волн и волн разрежения на изэнтропах и предполагает многократное использование итерационных методов для решения локальных задач, таких как нахождение точек перегиба на изэнтропах, точек касания прямой и кривой и т.д. При решении таких задач итерационными методами возникает проблема поиска начальных приближений, обеспечивающих сходимость метода. Предлагаемый в данной работе подход основан на табулировании точных решений задач Римана в широком диапазоне параметров начального состояния. Эти данные затем используются для нахождения приближенного решения без применения итерационных методов. Приближенный решатель был успешно применен для решения двух одномерных модельных задач о распаде разрыва в неклассической области.


Ключевые слова: задача Римана, неклассическая газовая динамика, точное решение, приближенное решение, геометрическая интерпретация решения, табулирование данных.

Получение: 26 февраля 2025 г. / Исправление: 5 апреля 2025 г. /
Принятие: 28 апреля 2025 г. / Публикация онлайн: 2 сентября 2025 г.

Математическое моделирование, численные методы и комплексы программ
Научная статья

© Коллектив авторов, 2025

© СамГТУ, 2025 (составление, дизайн, макет)

 Контент публикуется на условиях лицензии [Creative Commons Attribution 4.0 International](https://creativecommons.org/licenses/by/4.0/deed.ru) (<https://creativecommons.org/licenses/by/4.0/deed.ru>)

Образец для цитирования

Koroleva M. R. Approximate solution to the Riemann problem in non-classical gas dynamics, *Vestn. Samar. Gos. Tekhn. Univ., Ser. Fiz.-Mat. Nauki* [J. Samara State Tech. Univ., Ser. Phys. Math. Sci.], 2025, vol. 29, no. 3, pp. 503–515. EDN: ASUEIW. DOI: [10.14498/vsgtu2166](https://doi.org/10.14498/vsgtu2166).

Сведения об авторе

Мария Равиловна Королева  <https://orcid.org/0000-0001-5697-9199>

кандидат физико-математических наук; старший научный сотрудник; институт механики; e-mail: koroleva@udman.ru